Hindawi
Journal of Nanomaterials
Volume 2020, Article ID 5492953, 14 pages
https://doi.org/10.1155/2020/5492953

Research Article

Preparation of a Novel Thiol Surface Modifier and Fe_3O_4 Drug Loading Agent as well as Releasing under pH-Sensitivity

Wang Ya-zhen,[1,2,3] **Wu Xue-ying**,[1] **Di Yu-tao**,[1] **Lan Tian-yu**,[3,4] **and Zu Li-wu**[3,4]

[1]*College of Chemistry and Chemical Engineering, Qiqihar University, Qiqihar, 161006 Heilongjiang, China*
[2]*College of Chemistry, Chemical Engineering and Resource Utilization, Northeast Forestry University, Harbin, 150040 Heilongjiang, China*
[3]*Heilongjiang Province Key Laboratory of Polymeric Composition Material, Qiqihar University, Qiqihar, 161006 Heilongjiang, China*
[4]*College of Materials Science and Engineering, Qiqihar University, Qiqihar, 161006 Heilongjiang, China*

Correspondence should be addressed to Wang Ya-zhen; wyz6166@qqhru.edu.cn

Received 15 January 2020; Revised 12 March 2020; Accepted 23 March 2020; Published 8 May 2020

Guest Editor: Alessandro Dell'Era

In this paper, in order to take advantage of the combination between magnetic nano-Fe_3O_4 and surface modifier, a pH-sensitive drug delivery system that could effectively deliver doxorubicin (DOX) to tumor tissue was constructed. The novel drug delivery system named Fe_3O_4-TIPTS-g-(PEI-co-PEG) was prepared through three steps. The first step, a surface modifier with the thiol group, thiohydrazide-iminopropyltriethoxysilane surface modifier (named TIPTS), was synthesized for the first time. The second step, Fe_3O_4-TIPTS was synthesized by treating nano-Fe_3O_4 with TIPTS. The last step, Fe_3O_4-TIPTS-g-(PEI-co-PEG) was synthesized in the presence of the Fe_3O_4-TIPTS, polyethyleneimine (PEI), and polyethylene glycol (PEG) by mercapto-initiated radical polymerization. Among them, magnetic nanoparticles (MNPs) were used as magnetically responsive carriers, PEG was the surface-modifying compound, and PEI was the drug loading site which primary amine reacts with doxorubicin (DOX). Targeted nanoparticles were considerably stabilize in various physiological solutions and exhibited pH-sensitive performance in drug release. Thence, Fe_3O_4-TIPTS-g-(PEI-co-PEG) is a promising nanocarrier for targeting tumor therapy.

1. Introduction

In the last few decades, the incidence and mortality of malignancy increased year by year, and it has become the leading cause of death in humans. Chemotherapy [1] was the most commonly used clinical treatment for cancers. However, traditional anticancer drug formulations were nonspecificity [2] for tumors; especially when used in large doses, severe side effects were often caused [3]. That is why the development of efficient delivery systems with the ability to improve in vivo distribution and significant controlled sustained release behavior is required. One innovative technological approach to solve this problem is nanotechnology which focuses on the transfer of nano-sized biocompatible devices into the cells [4]. Among different types of nanomaterials, Fe_3O_4 nanoparticles is one kind of MNPs that have shown great promise as novel delivery systems and theranostics for personalized medicine due to their shape controllability and large specific surface area. And most importantly, their unique optical, electrical, and superparamagnetic properties give potential imaging development, targeted delivery, and synergistic drug therapy, suitable for drug delivery in cells [5]. Naked Fe_3O_4 NPs are easy to aggregate and oxidize and thus were often coated by hydrophilic materials and biocompatible polymers for targeted drug delivery [6–8].

The mercaptosilane surface modifier [9] is a particular kind of organosilicon compounds. The mercaptosilane surface modifier contains both a mercapto group reactive with an organic substance and a silicon functional group reactive with an inorganic substance. In view of this special molecular structure, a mercaptosilane surface modifier could be used as a "molecular bridge" [10] between organic substance and inorganic substance to prepare composite materials having excellent performances.

The surface coating [11] controls the absorption of particles by different cell types and affects biocompatibility, as well as the distribution of nanoparticles in the tissues of the organism [12–14], although many scientists use cationic bonds [15] to graft polymers onto the surface of nanoparticles as a drug carrier now. However, in the case of a pharmaceutical carrier obtained in this manner, cationic binding is extremely easily deactivated in physiological medium environment, resulting in poor stability. For this shortcoming, we use mercapto (-SH) [16] and polyethylene glycol (PEG) [17] propose for particle coating by free radical bonding, which can significantly improve the stability of nanoparticles in physiological medium environment, prolong the circulation time in the body, and improve the targeted delivery efficiency. PEG [18] in particular is considered to be a very promising material that protects the nanoparticles from the immune system, promotes a longer circulation time, and inhibits removal by the reticuloendothelial system. Although the application of polyethyleneimine (PEI) is plagued by their toxicity concerns, modification of PEI with PEG can address some of these concerns, improve the transfection efficiency, and enhance the systemic duration [19] at the same time.

Doxorubicin (DOX) is the most widely used chemotherapeutic drug. Although it has been standardized as an anticancer drug and has potential diverse toxicities, the clinical use of DOX is restricted [20]. In order to minimize the side effects, an efficient strategy is using nanoparticles as carriers for DOX delivery [21–23]. The novel drug delivery system in my manuscript is named as Fe_3O_4-TIPTS-g-(PEI-co-PEG). PEI and PEG were grafted Fe_3O_4 through TIPTS, which may load DOX to improve selective cytotoxicity of the drug to targeted cells and reduce the systemic toxicity to normal cells.

In normal tissues, the extracellular pH is relatively basic (pH = 7.4), whereas in tumor tissues, the pH is close to endosomes (pH = 5.0 – 6.0) or lysosomes (pH = 4.5 – 5.0) [24]. This difference provides a new idea for cancer treatment, which is to build a pH-sensitive drug delivery system. In the present paper, the $–NH_2$ group belonging to PEI of Fe_3O_4-TIPTS-g-(PEI-co-PEG) reacts with the -C=O group of DOX, and the resulting bond is the hydrazone bond. The hydrazone bond is kept stable in physiological condition; once the pH value decreases to 4.0–6.0, the hydrazone bond becomes unstable and then releases *massive drugs* [25, 26]. This pH-triggered delivery system will improve the efficacy of DOX while decreasing its cytotoxicity toward healthy cells (Scheme 1).

2. Experimental

2.1. Materials and Reagents. TIPTS were lab-made by ourselves. $FeCl_3{\cdot}6H_2O$, $FeCl_2{\cdot}4H_2O$, PEG [Mn = 2000], and DOX were purchased from Aladdin Industrial Corporation (Shanghai, China). PEI was purchased from Sigma-Aldrich Industrial Corporation (Shanghai, China). Ethanol was purchased from Tianjin Fuyu Chemical Corporation Limited (Tianjin, China). N-hexane and $NH_3{\cdot}H_2O$ was purchased from Tianjin Kemiou Chemical Reagent Corporation Limited (Tianjin, China). Methylbenzene was purchased from Aladdin Industrial Corporation (Shanghai, China). All of the chemicals were AR grade and were used as received without any purification. H_2O for laboratory experiments used was obtained after distillation.

2.2. Synthesis Procedure

2.2.1. Synthesis of Fe_3O_4 Nanoparticles. The coprecipitation method was used to prepare the Fe_3O_4 nanoparticles: $FeCl_3{\cdot}6H_2O$ (16.2 g) and $FeCl_2{\cdot}4H_2O$ (8.1 g) in a 1 : 2 molar ratio were dissolved in distilled water (175 ml) under nitrogen atmosphere with vigorous stirring. As the solution was heated to 70°C, $NH_3{\cdot}H_2O$ (28 wt%, 25 ml) was added dropwise to the solution until the pH of the solution is controlled at 10.0, under vigorous stirring, and the reaction was allowed to proceed for 5 h at 70°C. And then, the temperature was increased to 85°C to vapor the residual NH_3, then discard the excessive-iron ions by the magnetic separation procedure and filter. This part of the experiment process is shown in Scheme 2.

2.2.2. Synthesis of Thiol-Functionalized Fe_3O_4 Nanoparticles (Fe_3O_4-TIPTS). Fe_3O_4 nanoparticles were prepared by $FeCl_3{\cdot}6H_2O$ and $FeCl_2{\cdot}4H_2O$ in a coprecipitation method. Briefly, 25 ml methylbenzene and 1 g Fe_3O_4 nanoparticles were stirred at room temperature for 30 min. This was followed by the addition of 4 g TIPTS [27] (preparation of a lab-made novel thiol-containing silane coupling agent TIPTS was described in reference 39) and further stirring until dissolution was complete. Under purified N_2 atmosphere, this solution was heated to 65°C in a water bath, stirring for 8 h. Finally, the resulting product was filtered, washed with distilled methylbenzene for three times, and dried under vacuum for 24 h. This part of the experiment process is shown in Scheme 3.

2.2.3. Synthesis of Fe_3O_4-TIPTS-g-(PEI-co-PEG). Fe_3O_4-TIPTS (1.77 g) was dissolved in 50 ml methylbenzene and stirred at room temperature for 30 min. Followed by the addition of 4.425 g PEI dissolved in 10 ml ethanol and 10 g PEG dissolved in 20 ml methylbenzene. This solution was heated to 55°C in a water bath, continuous flow of nitrogen into the stream, stirring for 8 h. Finally, the resulting product was filtered, washed with distilled water for three times, and dried under vacuum for 24 h. This part of the experiment process is shown in Scheme 4.

2.2.4. Drug Loading. To load DOX on modified MNPs, 20 mg dry Fe_3O_4-TIPTS-g-(PEI-co-PEG) was dispersed in 8 ml DMSO; 3 mg DOX was added and allowed to react with the nanoparticles for 24 h in the dark. The resulted products were collected by magnetic decantation and washed twice with deionized water. The DOX-loaded Fe_3O_4-TIPTS-g-(PEI-co-PEG) were freeze-dried and stored in the dark at 4°C. The amount of unbound DOX was quantified using a UV-Vis spectrophotometer at 420 nm.

2.2.5. In Vitro Release Studies. Briefly, 0.01 M phosphate buffer solution (PBS) was prepared at three different pH values (4.5, 5.5, and 7.4) which each pH was chosen to imitate

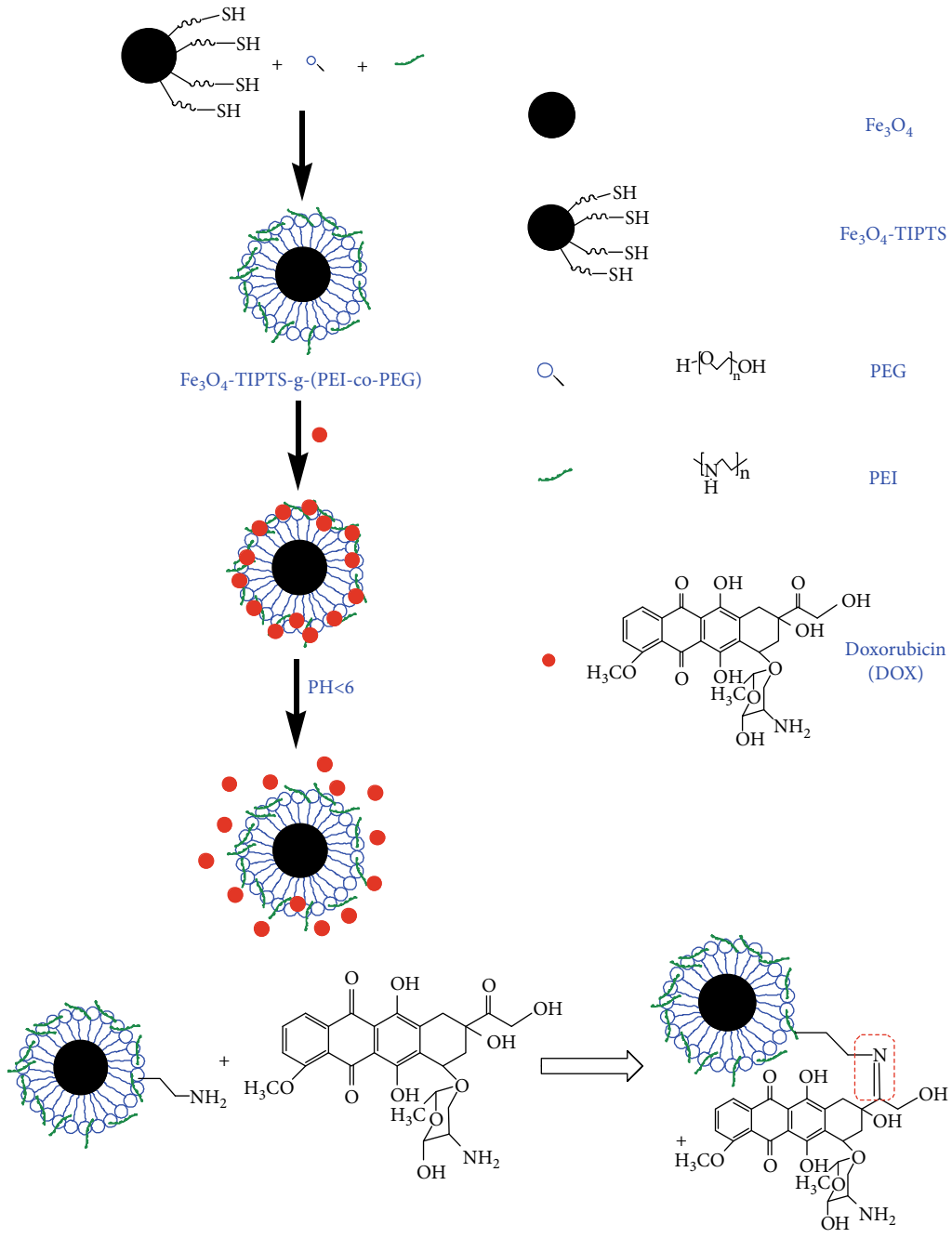

Scheme 1: Outline for the preparation of Fe_3O_4-TIPTS-g-(PEI-co-PEG), drug loading, and in vitro release studies.

$$2FeCl_3 + FeCl_2 + 4H_2O + 8NH_3 \longrightarrow Fe_3O_4 + 8NH_4Cl$$

Scheme 2: The preparation of Fe_3O_4 nanoparticles.

conditions either within tumors or within normal tissues. 10 mg DOX-loaded Fe_3O_4-TIPTS-g-(PEI-co-PEG) was dispersed in 3 ml PBS and then transferred to a dialysis bag that was immersed in 50 ml of the same medium. At selected time intervals, 3 ml PBS outside the dialysis bag was removed for analysis and replaced by the same volume of fresh PBS. The release experiments of each pH were conducted in triplicate.

2.3. Characterization. The samples compressed with KBr were analyzed by a FTIR spectrometer (Spectrum Two, PerkinElmer Company of United States of America) at room temperature, the spectral range was 450-4000 cm^{-1}, and the spectral resolution was 4 cm^{-1}. The X-ray intensity was measured in the range of $10° < 2\theta < 80°$ with a scan speed of 2θ/min. A Beckman Coulter LS-880 Laser Diffraction Particle Size analyzer was used in this study. Its measuring range was 0.01 μm to 2000 μm. With its PIDS (Polarization Intensity Differential Scattering) assembly, lower size limit could be extended to as low as 0.04 μm. X-ray powder diffraction (XRD) analysis was performed using Rigaku Dmax2200PC

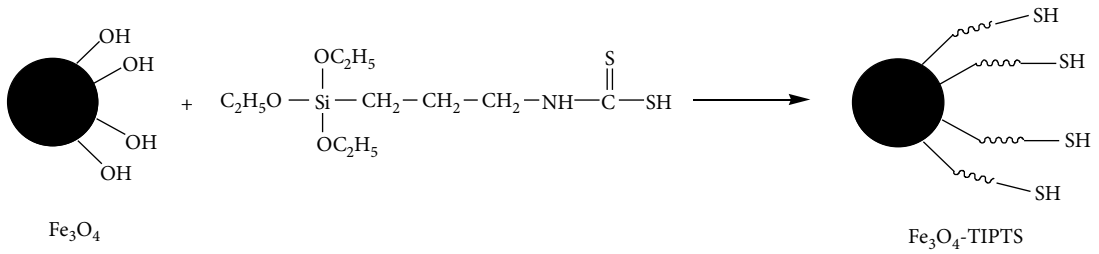

Scheme 3: The preparation of Fe_3O_4-TIPTS.

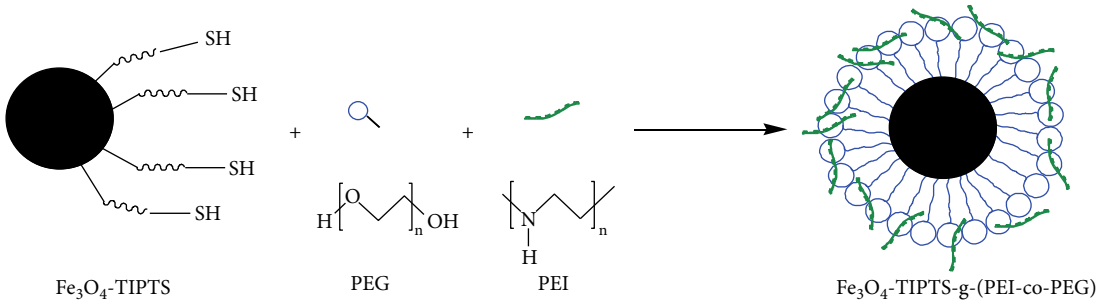

Scheme 4: The preparation of Fe_3O_4-TIPTS-g-(PEI-co-PEG).

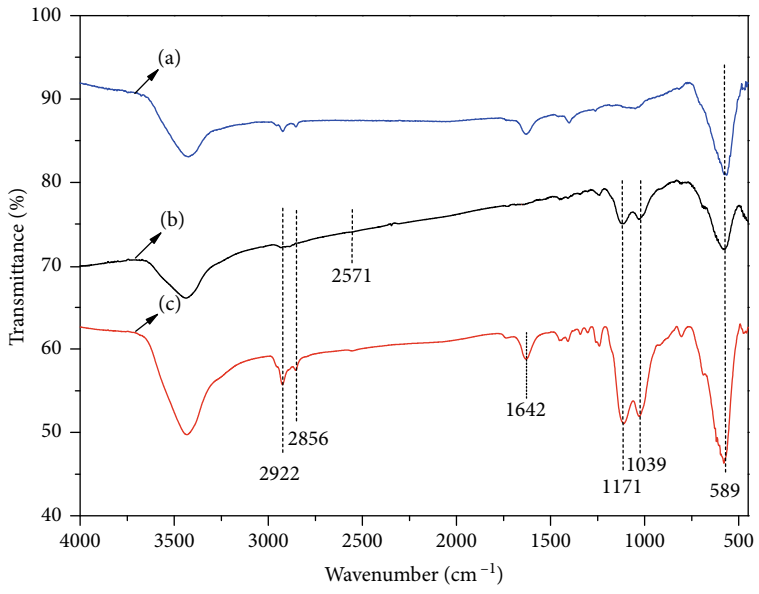

Figure 1: FTIR spectra of products. (a) Fe_3O_4. (b) Fe_3O_4-TIPTS. (c) Fe_3O_4-TIPTS-g-(PEI-co-PEG).

diffractometer (Rigaku Corporation, Tokyo, Japan) and Cu K-radiation. The magnetic properties of the products were determined by a vibrating sample magnetometer (VSM) (VL-072, Quantum Design Company of United States of America). UV-vis spectra were measured on a UV-vis spectrometer (Lambda 35, PerkinElmer Company of United States of America).

3. Results and Discussion

3.1. The Preparation of Fe_3O_4-TIPTS-g-(PEI-co-PEG)

3.1.1. FTIR Analysis. FTIR spectra of products are shown in Figure 1. From these curves, the peak could be seen at 589 cm^{-1} attributed to the stretching vibration of the Fe-O group, the peak could be seen at 1039 cm^{-1} attributed to the stretching vibration of the C-H group, the peak could be seen at 1171 cm^{-1} attributed to the C-C group, the peak could be seen at 1642 cm^{-1} attributed to the C-OH group, the peak could be seen at 2571 cm^{-1} attributed to the -SH group, and the peak could be seen at 2856 cm^{-1} and 2922 cm^{-1} attributed to the stretching vibration of the $-CH_2$ group.

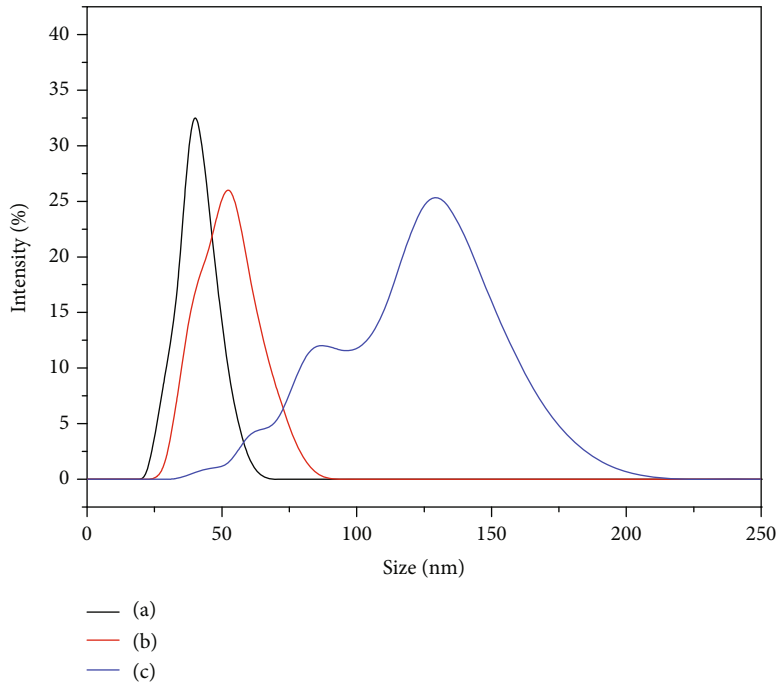

Figure 2: The particle size spectra of products. (a) Fe_3O_4. (b) Fe_3O_4-TIPTS. (c) Fe_3O_4-TIPTS-g-(PEI-co-PEG).

From curve (a), curve (b) and curve (c), the peak at 2856 cm^{-1} and 2922 cm^{-1} could only be seen at curve (b) and curve (c), not at curve (a), because TIPTS and copolymer could make nano-Fe_3O_4 organized. The peak at 2571 cm^{-1} could only be seen at curve (b), because the -SH group was decomposed to obtain free radicals for grafting two polymers on Fe_3O_4-TIPTS. The peak at 1642 cm^{-1} could only be seen at curve (b), because the C-OH group belongs to PEI, which further indicated that polymers were successful to be grafted on Fe_3O_4-TIPTS.

3.1.2. Particle Size Analysis. The particle size spectra for Fe_3O_4, Fe_3O_4-TIPTS and Fe_3O_4-TIPTS-g-(PEI-co-PEG) are shown in Figure 2. The results showed that the diameter size of Fe_3O_4 was 39.6 nm, the diameter size of Fe_3O_4-TIPTS was 47.6 nm, and the diameter size of Fe_3O_4-TIPTS-g-(PEI-co-PEG) was 112.8 nm. It indicated that the diameter size of the latter one is gradually larger than the diameter size of the previous one, because TIPTS by lab-made could modify Fe_3O_4 in a smooth way. Moreover, TIPTS could also obtain free radicals for grafting PEI and PEG onto the surface of Fe_3O_4-TIPTS. And then, the diameter size results of all products were between 20 and 150 nm, which is beneficial to the absorption of endothelial reticular system and recognition of phagocytic cells.

3.1.3. XRD Analysis. The XRD spectra for the products for Fe_3O_4 and Fe_3O_4-TIPTS-g-(PEI-co-PEG) are shown in Figure 3. The crystal lattice change of Fe_3O_4 upon grafting of PEI and PEG was investigated using XRD analysis. The Fe_3O_4 exhibited several sharp peaks at 18.21 (1 1 1), 29.96 (2 2 0), 35.28 (3 1 1), 42.88 (4 0 0), 53.18 (4 2 2), 56.69 (5 1 1), 62.25 (4 4 0), and 74.62 (6 2 2), respectively, as shown in

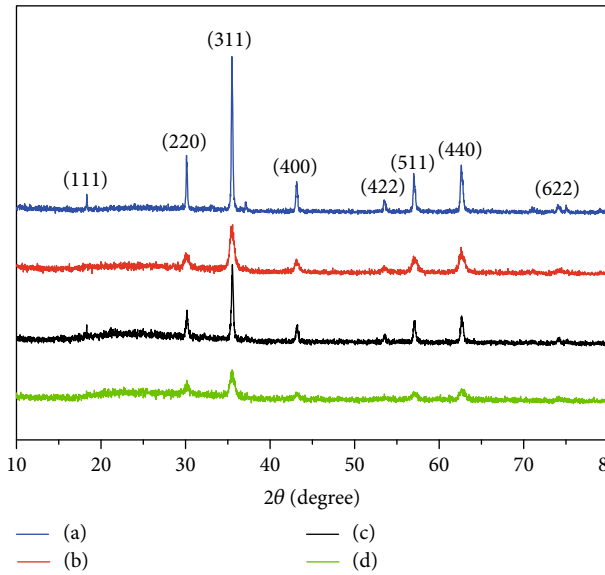

Figure 3: XRD spectra of products. (a) Fe_3O_4. (b) Fe_3O_4-TIPTS. (c) Fe_3O_4-TIPTS -g-(PEI-co-PEG). (d) Loading DOX onto Fe_3O_4-TIPTS-g-(PEI-co-PEG).

Figure 3. The broad peak from 17.58 to 31.88 of the XRD curve showed that PEI and PEG prepared in the absence of Fe_3O_4 was amorphous. The reflection peaks of Fe_3O_4-TIPTS-g-(PEI-co-PEG) could all be ascribed to the crystal planes of Fe_3O_4. The broad weak diffraction peak of PEI and PEG did not affect the crystal lattice of Fe_3O_4. This observation indicated that the composite sample had a still ordered arrangement than PEI and PEG owing to the inclusion of Fe_3O_4. The performance which was targetable drug delivery of Fe_3O_4 was not affected by the grafted polymer.

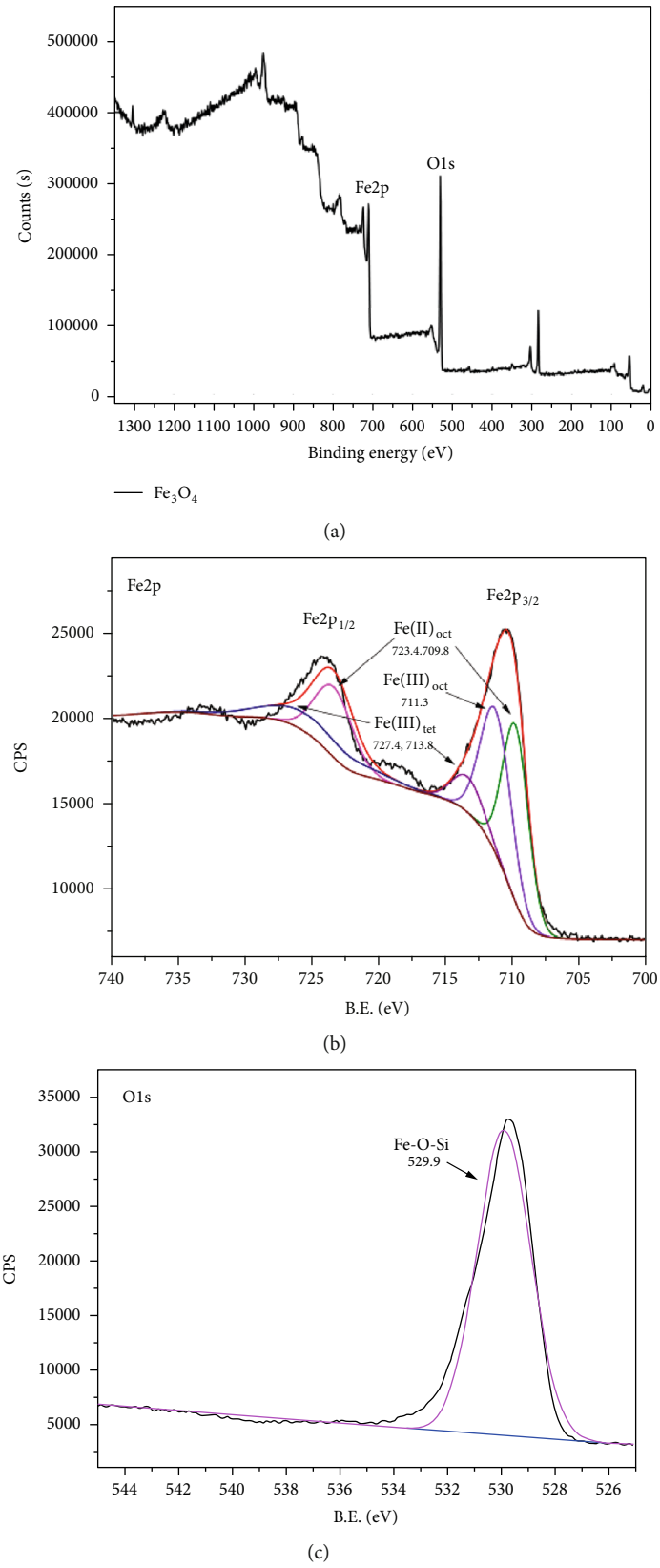

Figure 4: XPS spectra of Fe_3O_4. (a) Full spectrum of Fe_3O_4. (b) Peak separation of Fe. (c) Peak separation of O.

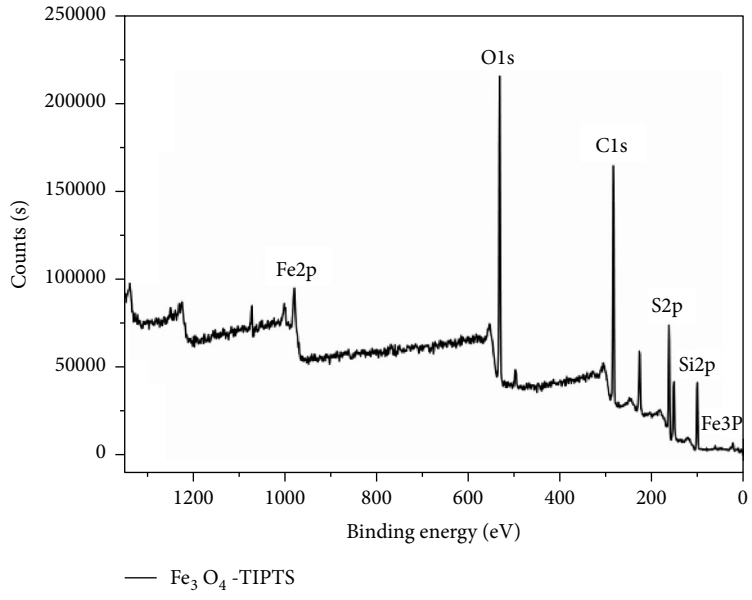

(a)

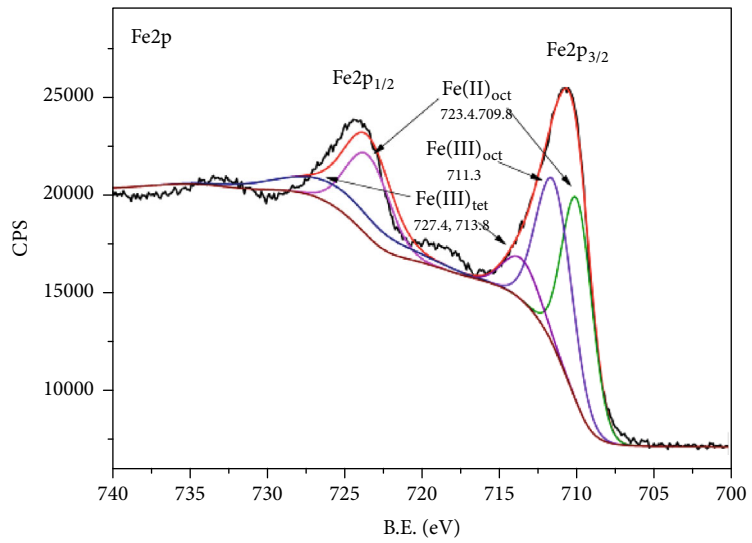

(b)

Figure 5: Continued.

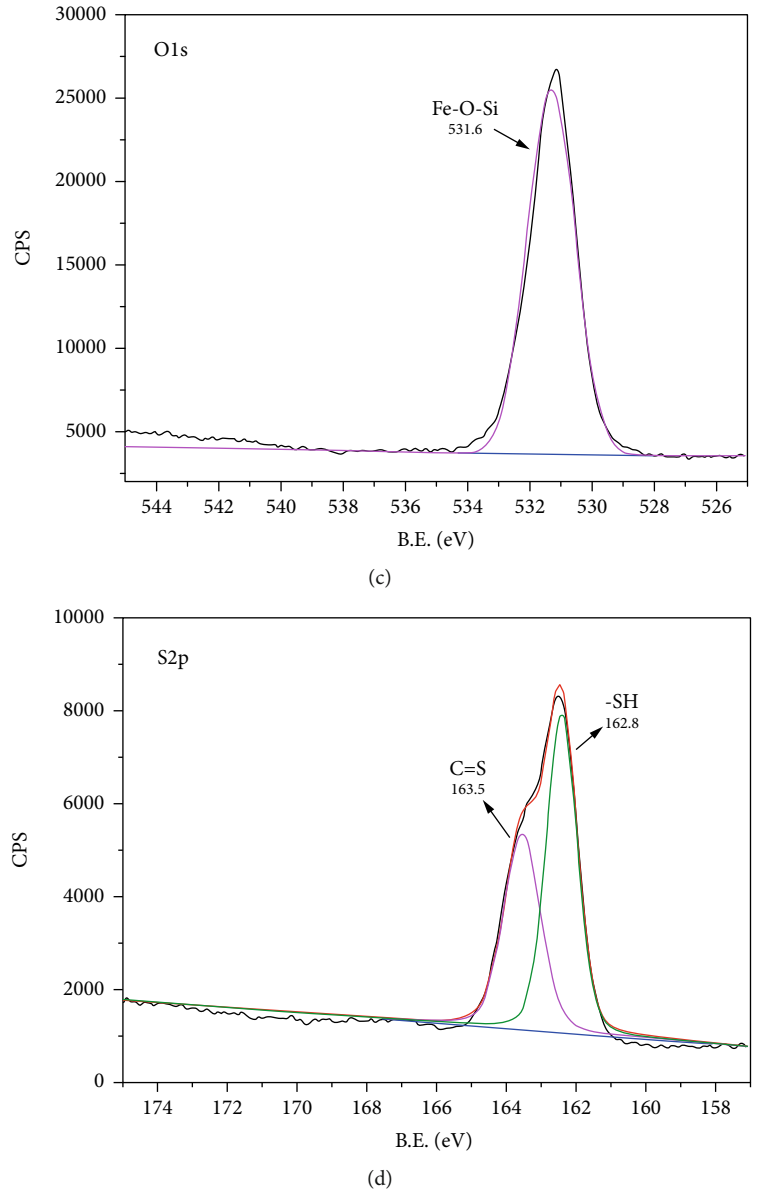

Figure 5: XPS spectra of Fe_3O_4-TIPTS. (a) Full spectrum of Fe_3O_4-TIPTS. (b) Peak separation of Fe. (c) Peak separation of O. (d) Peak separation of S.

3.1.4. XPS Analysis. From Figures 4–6, it separately showed XPS spectra of Fe_3O_4, Fe_3O_4-TIPTS, and Fe_3O_4-TIPTS-g-(PEI-co-PEG). Every full spectra contained all the distinct peaks of the elements, and the location was accurate. Peak separation of each element was obtained by peak separation and fitting for each element. Every peak separation by Fe of Fe_3O_4, Fe_3O_4-TIPTS, and Fe_3O_4-TIPTS-g-(PEI-co-PEG) was exactly the same. Every peak separation by S and O of Fe_3O_4, Fe_3O_4-TIPTS and Fe_3O_4-TIPTS-g-(PEI-co-PEG) appeared different, but the fitting results are consistent with the whole curve. The above results further prove that the structure of Fe_3O_4, Fe_3O_4-TIPTS and Fe_3O_4-TIPTS-g-(PEI-co-PEG) prepared by the experiment were accurate.

3.1.5. VSM Analysis. Neither the remanence nor the coercivity was observed in the three hysteresis curves; therefore, the magnetization results shown in Figure 7 suggested that Fe_3O_4-TIPTS-g-(PEI-co-PEG) was indeed superparamagnetic and had a strong magnetic response. They exhibited superparamagnetism with the saturation magnetization (Ms) values of 68.23, 63.58, and 55.22 emu/g at 25°C, respectively. It indicated that the polymerization did not affect the magnetic properties of the superparamagnetic nanoparticles because the structure of the Fe_3O_4 nanoparticles remained in the polymerization procedure. Therefore, the DOX-loaded Fe_3O_4-TIPTS-g-(PEI-co-PEG) can be easily controlled by an external magnetic field to accurately deliver DOX to the target area. Furthermore, the decrease in the saturation magnetization of the Fe_3O_4-TIPTS and Fe_3O_4-TIPTS-g-(PEI-co-PEG) nanoparticles compared with the Fe_3O_4 was ascribed to the TIPTS and the copolymer of PEI and PEG ingredients grafted.

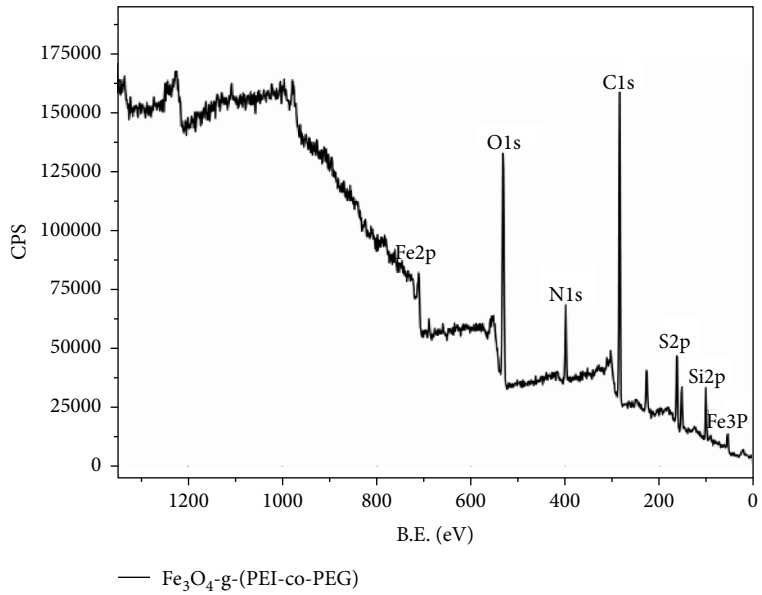

(a)

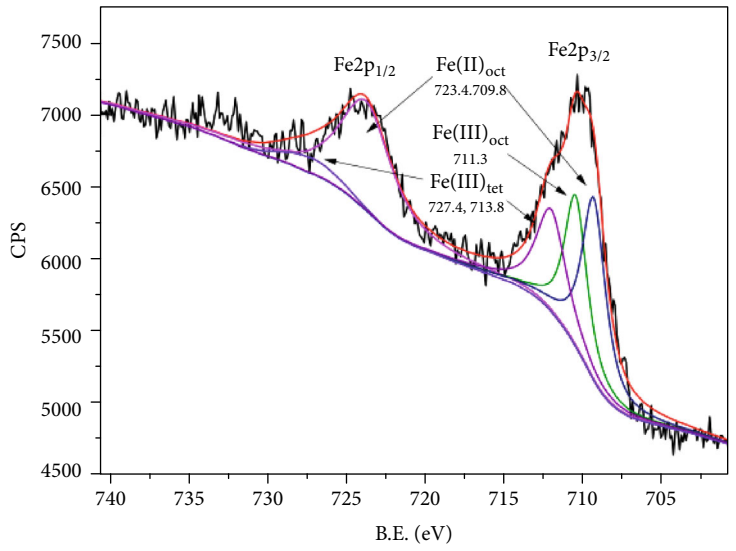

(b)

Figure 6: Continued.

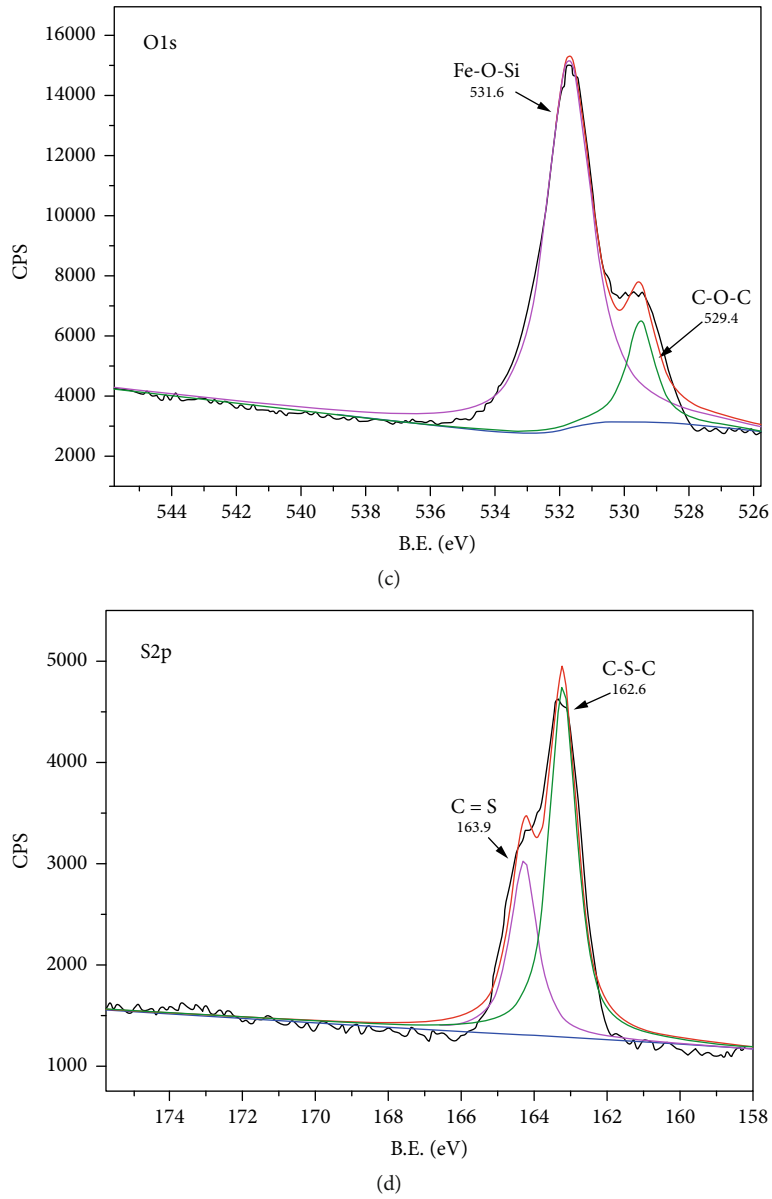

Figure 6: XPS spectra of Fe_3O_4-TIPTS-g-(PEI-co-PEG). (a) Full spectrum of Fe_3O_4-TIPTS-g-(PEI-co-PEG). (b) Peak separation of Fe. (c) Peak separation of O. (d) Peak separation of S.

3.1.6. SEM Analysis. From Figure 8, it showed SEM images of Fe_3O_4, Fe_3O_4-TIPTS, and Fe_3O_4-TIPTS-g-(PEI-co-PEG), respectively. From Figure 8(a), the Fe_3O_4 synthesized by the method in this paper presented a uniform particle size, and each nano-microsphere is basically in an independent state. Figure 8(b) shows the higher magnification image of Fe_3O_4-TIPTS; it could be seen that TIPTS (a silane surface modifier with thiols group) was grafted on the surface of Fe_3O_4. Figure 8(c) shows the higher magnification image of Fe_3O_4-TIPTS-g-(PEI-co-PEG). Under the action of a mercapto group, branching and cluster polymers were formed by PEI and PEG grafted onto Fe_3O_4. And then, the particle size of Fe_3O_4-TIPTS-g-(PEI-co-PEG) was uneven due to the difference in the amount of the graft polymer.

3.2. Drug Loading and In Vitro Release Studies

3.2.1. FTIR Analysis. FTIR spectra of DOX and DOX-loaded Fe_3O_4-TIPTS-g-(PEI-co-PEG) are shown in Figure 9. From these curves, the peak could be seen at 558 cm^{-1} attributed to the stretching vibration of the Fe-O group, the peak could be seen at 2851 cm^{-1} and 2920 cm^{-1} attributed to the stretching vibration of the -CH_2 group, the peak at 3332 cm^{-1} could be attributed to the O–H groups of PEG and DOX. The peaks at 1617 cm^{-1} could be attributed to N–H bending. The peaks at 1280 cm^{-1} could be attributed to C–N stretching modes. The peaks at 1408 cm^{-1} could be attributed to quinine. The peaks at 1,285 cm^{-1} could be attributed to anthracycline. The peaks at 1730 cm^{-1} could be attributed to 13-carbonyl

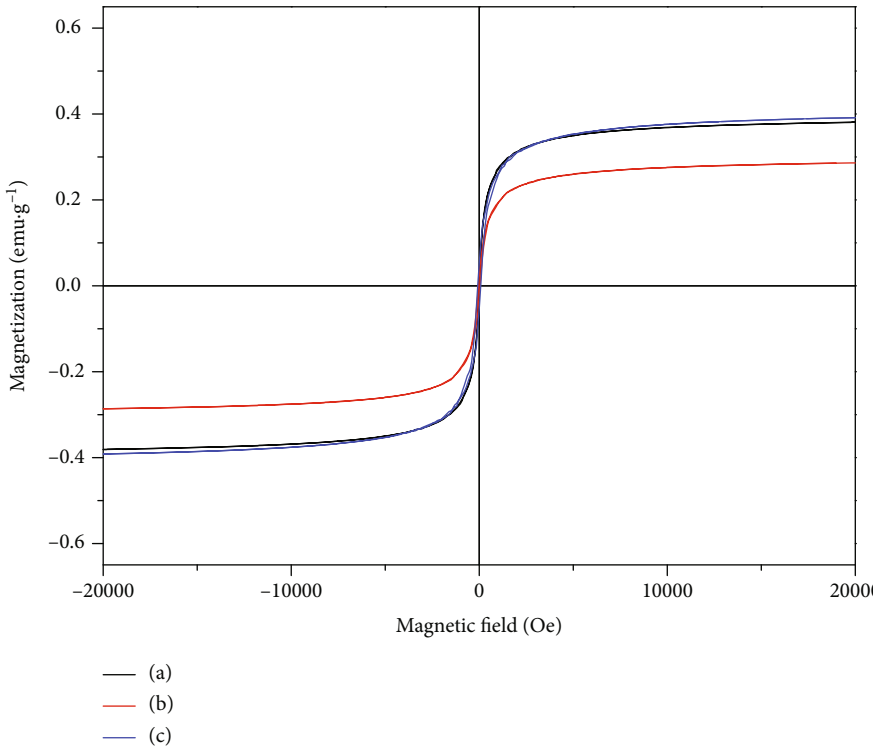

Figure 7: VSM measurements. (a) Fe_3O_4; (b) Fe_3O_4-TIPTS; (c) Fe_3O_4-TIPTS-g-(PEI-co-PEG).

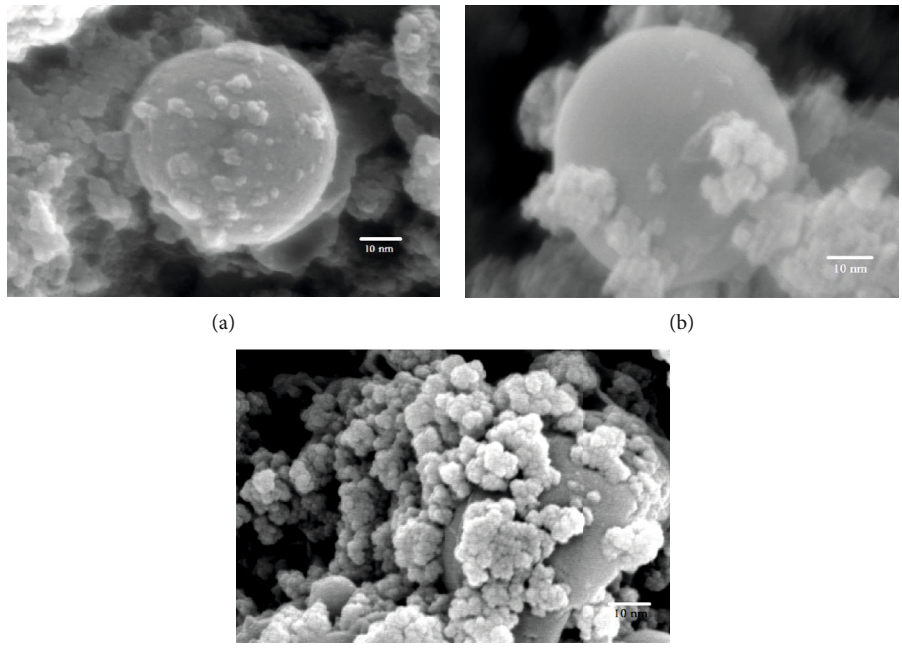

Figure 8: SEM images of the products. (a) Fe_3O_4; (b) Fe_3O_4-TIPTS; (c) Fe_3O_4-TIPTS-g-(PEI-co-PEG).

moieties. 1343 cm^{-1} could be attributed to hydrazone bond. The quinone, anthracycline, and 13-carbonyl moieties were all in DOX. Through comparison, the peak at 1730 cm^{-1} does not appear in DOX-loaded Fe_3O_4-TIPTS-g-(PEI-co-PEG) and the peak at 1343 cm^{-1} was the characteristic peak only appear in the curve of DOX-loaded Fe_3O_4-TIPTS-g-(PEI-co-PEG). In summary, DOX was successfully loaded onto Fe_3O_4-TIPTS-g-(PEI-co-PEG).

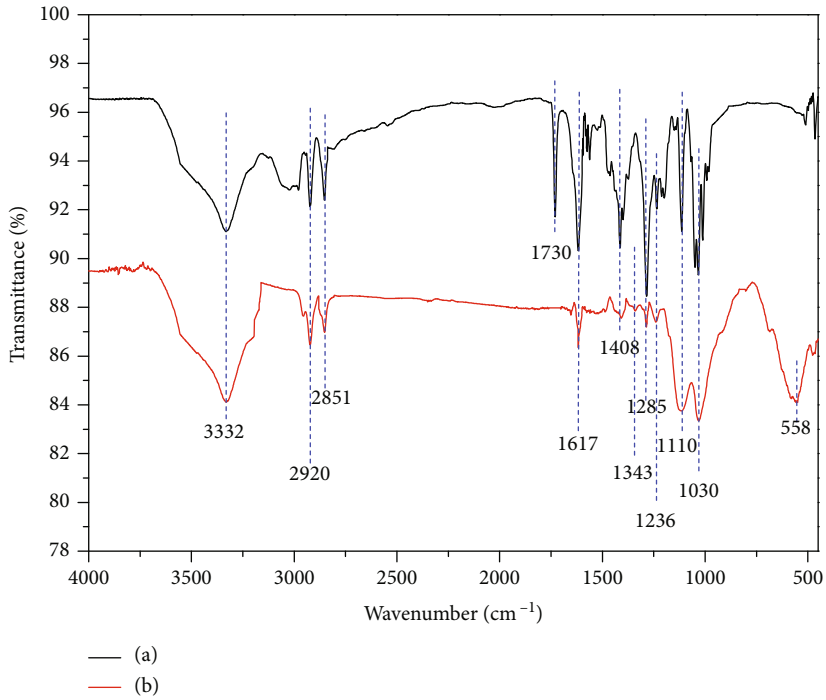

Figure 9: FTIR spectra of products. (a) DOX; (b) DOX-loaded Fe_3O_4-TIPTS-g-(PEI-co-PEG).

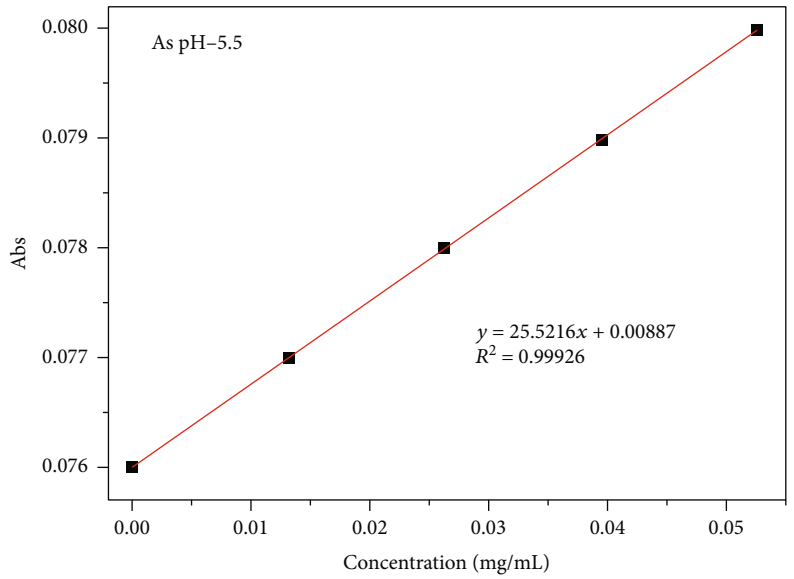

Figure 10: Standard curve of vitro release of DOX.

3.2.2. In Vitro Release Studies. The results of vitro release are shown in Figure 10. In vitro release studies of DOX over time were studied by monitoring the absorbance at 482 nm. In vitro release of DOX from Fe_3O_4-TIPTS-g-(PEI-co-PEG) was simulated at 37°C. Standard curve was calculated at pH 5.5. The relationship between the absorption value (Abs) and the concentration is derived according to

$$\mathrm{Abs} = \left(\mathrm{V} * c_1 + \mathrm{V}^{\cdot} * \Sigma c_{\mathrm{i}}\right) / m_{\mathrm{drug}}. \quad (1)$$

Thus, the standard curve of vitro release of DOX was

$$y = 25.5216\mathrm{x} + 0.00887 \left(R^2 = 0.99926\right). \quad (2)$$

The result of pH sensitive about vitro release of DOX is shown in Figure 11. It indicated that DOX onto Fe_3O_4-TIPTS-g-(PEI-co-PEG) was relatively stable at blood pH and more effectively released its payload at pH = 4.5 than pH = 5.5 or pH = 7.4. The functionalized particles slowly released DOX over 80 h at 37°C under pH 4.5 (lysosomes),

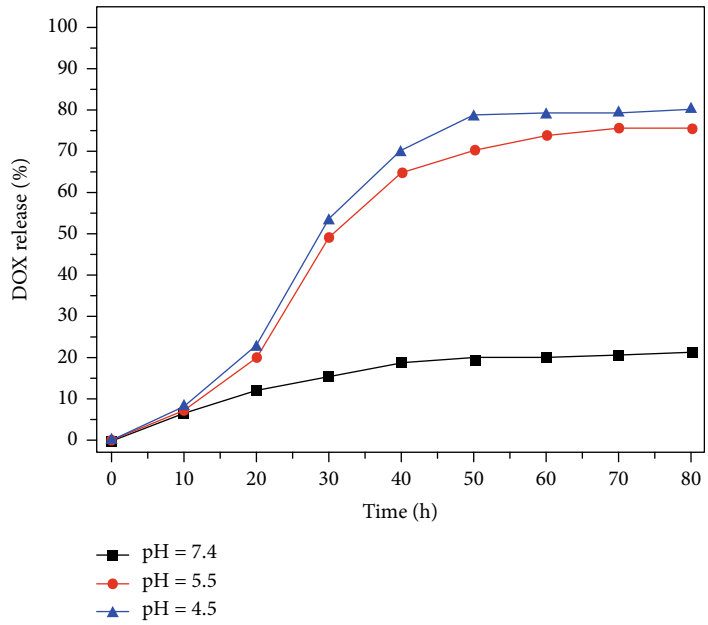

Figure 11: In vitro release of DOX at pH 4.5, 5.5, and 7.4.

5.5 (endosomes), and 7.4(normal tissues) PBS solutions, which was both time- and pH-dependent; the cumulative dissolution profiles of nanoparticles are shown in Figure 11. It indicated that only 21.06% of drug was released from Fe_3O_4-TIPTS-g-(PEI-co-PEG) at pH 7.4, separately, over the process of 80 h, while at pH 5.5, it demonstrated higher release satisfied with 75.68% and at pH = 4.5 up to 80.24%. The result indicated that nanoparticles under acidic conditions showed higher DOX release rates at endosomal pH (4.5–5.5) as compared with normal tissues pH (7.4). This phenomenon could be attributed to the fact that after placing Fe_3O_4-TIPTS-g-(PEI-co-PEG) in acidic PBS, the C=N bond between DOX and Fe_3O_4-TIPTS-g-(PEI-co-PEG) is attacked by H^+, releasing DOX. While from pH 5.5 to 4.5, the release rate of DOX was also increased slightly. This phenomenon was due to the protonation of the DOX amino group, which could gave DOX a positive charge to enhance its solubility in acidic conditions; accordingly, a faster drug release was caused.

4. Conclusion

In summary, our research results have synthesized a DOX-loaded pH-sensitive magnetic system for targeted drug delivery. Nano-Fe_3O_4 was modified by the mercaptosilane surface modifier TIPTS, and block copolymer poly(ethylene glycol-co-ethyleneimine) grafted Fe_3O_4 to obtain Fe_3O_4-TIPTS-g-(PEI-co-PEG). The nano-Fe_3O_4 was a core of Fe_3O_4-TIPTS-g-(PEI-co-PEG) which possesses the targeted function. DOX was bonded with Fe_3O_4-TIPTS-g-(PEI-co-PEG) by a hydrazone bond. At different pH, the hydrazone bond could act as the switch to control the release of the drug encapsulated, so the potential of DOX-loaded Fe_3O_4-TIPTS-g-(PEI-co-PEG) as the carrier for pH-sensitive drug release is demonstrated. In vitro, DOX was released more readily at pH 4.5, which 80.24% DOX was released within 80 h. Therefore, the results demonstrate the versatility of the DOX-loaded magnetic nanoparticles as a potential anti-tumor drug delivery system.

Data Availability

The data used to support the findings of this study are available from the corresponding author upon request.

Conflicts of Interest

No potential conflict of interest was reported by the authors.

Acknowledgments

The authors are grateful for support from the National Natural Science Foundation of China (grant number: 21376127), the Scientific Research Projects Foundation of Heilongjiang Education Department (grant number: YSTSXK201860), and the Fundamental Research Funds in Heilongjiang Provincial Universities (grant number: 135309110).

References

[1] J. Xi, L. Da, C. Yang et al., "Mn^{2+}-coordinated PDA@-DOX/PLGA nanoparticles as a smart theranostic agent for synergistic chemo-photothermal tumor therapy," *International Journal of Nanomedicine*, vol. 12, pp. 3331–3345, 2017.

[2] U. Sang Shin, J. W. Seo, B. Kundu, H. W. Kim, and M. Eltohamy, "Super-magnetic smart hybrid doxorubicin loaded nanoparticles effectively target breast adenocarcinoma cells," *Microporous and Mesoporous Materials*, vol. 243, pp. 206–213, 2017.

[3] F. Farvadi, A. M. Tamaddon, Z. Sobhani, and S. S. Abolmaali, "Polyionic complex of single-walled carbon nanotubes and

PEG-grafted-hyperbranched polyethyleneimine (PEG-PEI-SWNT) for an improved doxorubicin loading and delivery: development andin vitrocharacterization," *Artificial Cells, Nanomedicine, and Biotechnology*, vol. 45, no. 5, pp. 855–863, 2017.

[4] R. Klingeler, S. Hampel, and B. Büchner, "Carbon nanotube based biomedical agents for heating, temperature sensoring and drug delivery," *International Journal of Hyperthermia*, vol. 24, no. 6, pp. 496–505, 2009.

[5] L. Huang, L. Ao, W. Wang, D. Hu, Z. Sheng, and W. Su, "Multifunctional magnetic silica nanotubes for MR imaging and targeted drug delivery," *Chemical Communications*, vol. 51, no. 18, pp. 3923–3926, 2015.

[6] H. Song, F. Quan, Z. Yu et al., "Carboplatin prodrug conjugated Fe_3O_4 nanoparticles for magnetically targeted drug delivery in ovarian cancer cells," *Journal of Materials Chemistry B*, vol. 7, no. 3, pp. 433–442, 2019.

[7] A. Nordborg, F. Limé, A. Shchukarev, and K. Irgum, "A cation-exchange material for protein separations based on grafting of thiol-terminated sulfopropyl methacrylate telomers onto hydrophilized monodisperse divinylbenzene particles," *Journal of Separation Science*, vol. 31, no. 12, pp. 2143–2150, 2008.

[8] A. Beiraghi, K. Pourghazi, and M. Amoli-Diva, "Au nanoparticle grafted thiol modified magnetic nanoparticle solid phase extraction coupled with high performance liquid chromatography for determination of steroid hormones in human plasma and urine," *Analytical Methods*, vol. 6, no. 5, pp. 1418–1426, 2014.

[9] A. H. M. Yusoff, N. S. Midhat, and F. J. Mohd, "Synthesis and characterization of biocompatible Fe_3O_4 nanoparticles at different pH," *Advanced Materials Technologies*, vol. 1835, no. 1, article 020010, 2017.

[10] S. Davaran, D. Asgari, S. Davaran et al., "Preparation and in vitro evaluation of doxorubicin-loaded Fe_3O_4 magnetic nanoparticles modified with biocompatible copolymers," *International Journal of Nanomedicine*, vol. 7, pp. 511–526, 2012.

[11] L. Sun, J. Wang, and Z. Wang, "Recognition and transmembrane delivery of bioconjugated Fe_2O_3@au nanoparticles with living cells," *Nanoscale*, vol. 2, no. 2, pp. 269–276, 2010.

[12] D. Li, M. Hua, K. Fang, and R. Liang, "BSA directed-synthesis of biocompatible Fe_3O_4 nanoparticles for dual-modal T_1 and T_2 MR imaging *in vivo*," *Analytical Methods*, vol. 9, no. 21, pp. 3099–3104, 2017.

[13] J. Yang, M. Pan, R. Shi et al., "Novel Fe_3O_4 Hollow microspheres: nontemplate hydrothermal synthesis, superparamagnetism and biocompatibility," *Nanoscience and Nanotechnology Letters*, vol. 9, no. 2, pp. 109–117, 2017.

[14] D. Li, M. Deng, Z. Yu et al., "Biocompatible and stable GO-coated Fe_3O_4 Nanocomposite: a robust drug delivery carrier for simultaneous tumor MR imaging and targeted therapy," *ACS Biomaterials Science & Engineering*, vol. 4, no. 6, pp. 2143–2154, 2018.

[15] Z. Li, X. Liu, X. Chen, M. X. Chua, and Y. L. Wu, "Targeted delivery of Bcl-2 conversion gene by MPEG-PCL-PEI-FA cationic copolymer to combat therapeutic resistant cancer," *Materials Science And Engineering: C*, vol. 76, pp. 66–72, 2017.

[16] H. Shao, J. Qi, T. Lin, Y. Zhou, and F. Yu, "Characterization of Fe_3O_4@CS@NMDP magnetic nanoparticles with core–shell structure prepared by chemical cross-linking method," *Functional Materials Letters*, vol. 10, no. 5, article 1750056, 2017.

[17] J. V. Jokerst, T. Lobovkina, R. N. Zare, and S. Gambhir, "Nanoparticle PEGylation for imaging and therapy," *Nanomedicine*, vol. 6, no. 4, pp. 715–728, 2011.

[18] Y. Fang, J. Xue, S. Gao et al., "Cleavable PEGylation: a strategy for overcoming the "PEG dilemma" in efficient drug delivery," *Drug Delivery*, vol. 24, no. 2, pp. 22–32, 2017.

[19] H. Danafar, A. Sharafi, H. Kheiri Manjili, and S. Andalib, "Sulforaphane delivery using mPEG–PCL co-polymer nanoparticles to breast cancer cells," *Pharmaceutical Development and Technology*, vol. 22, no. 5, pp. 642–651, 2017.

[20] A. Pugazhendhi, T. N. J. I. Edison, B. K. Velmurugan, J. A. Jacob, and I. Karuppusamy, "Toxicity of doxorubicin (Dox) to different experimental organ systems," *Life Sciences*, vol. 200, pp. 26–30, 2018.

[21] M. I. Majeed, Q. Lu, W. Yan et al., "Highly water-soluble magnetic iron oxide (Fe_3O_4) nanoparticles for drug delivery: enhanced in vitro therapeutic efficacy of doxorubicin and MION conjugates," *Journal Of Materials Chemistry B*, vol. 1, no. 22, pp. 2874–2884, 2013.

[22] C. H. Fan, Y. H. Cheng, C. Y. Ting et al., "Ultrasound/magnetic targeting with SPIO-DOX-microbubble complex for image-guided drug delivery in brain tumors," *Theranostics*, vol. 6, no. 10, pp. 1542–1556, 2016.

[23] X. Jia, Z. Yang, Y. Wang et al., "Hollow mesoporous silica@-metal–organic framework and applications for pH-responsive drug delivery," *ChemMedChem*, vol. 13, no. 5, pp. 400–405, 2018.

[24] Z. Zhou, F. Hu, S. Hu et al., "pH-activated nanoparticles with targeting for the treatment of oral plaque biofilm," *Journal of Materials Chemistry B*, vol. 6, no. 4, pp. 586–592, 2018.

[25] M. Huan, B. Zhang, Z. Teng et al., "In vitro and in vivo antitumor activity of a novel pH-activated polymeric drug delivery system for doxorubicin," *PLoS One*, vol. 7, no. 9, article e44116, 2012.

[26] W. Chen, F. Meng, R. Cheng, and Z. Zhong, "pH-sensitive degradable polymersomes for triggered release of anticancer drugs: a comparative study with micelles," *Journal of Controlled Release Official Journal of the Controlled Release Society*, vol. 142, no. 1, pp. 40–46, 2010.

[27] W. Xue-Ying, W. Ya-Zhen, D. Yu-Tao, L. Tian-Yu, and Z. Li-Wu, "Preparation and thermal decomposition kinetics of novel silane coupling agent with mercapto group," *Journal of Nanomaterials*, vol. 2019, Article ID 6089065, 9 pages, 2019.